Conservation Physiology

Volume 8 • 2020 10.1093/conphys/coaa060

SEB SOCIETY FOR EXPERIMENTAL BIOLOGY

Research article

Can the carbon and nitrogen isotope values of offspring be used as a proxy for their mother's diet? Using foetal physiology to interpret bulk tissue and amino acid δ^{15}N values

Nico Lübcker[1,*], John P. Whiteman[2,3], Seth D. Newsome[3], Robert P. Millar[4,5], P. J. Nico de Bruyn[1]

[1]Department of Zoology and Entomology, Mammal Research Institute, University of Pretoria, Private Bag X20, Hatfield, Pretoria, 0028, South Africa
[2]Department of Biological Sciences, Old Dominion University, 5115 Hampton Boulevard, Norfolk, VA, 23529, USA
[3]Department of Biology, University of New Mexico, Albuquerque, NM, 87131, USA
[4]Centre for Neuroendocrinology and Department of Immunology, Faculty of Health Sciences, University of Pretoria, Pretoria, 0001, South Africa
[5]Department of Integrative Biomedical Sciences, Neurosciences Institute and Institute of Infectious Diseases and Molecular Medicine, University of Cape Town, Anzio Road, Observatory 7925, South Africa

***Corresponding author:** Department of Zoology and Entomology, Mammal Research Institute,University of Pretoria, Private Bag X20, Hatfield, Pretoria, 0028, South Africa. Email: nlubcker@zoology.up.ac.za

The measurement of bulk tissue nitrogen (δ^{15}N) and carbon isotope values (δ^{13}C) chronologically along biologically inert tissues sampled from offspring can provide a longitudinal record of their mothers' foraging habits. This study tested the important assumption that mother–offspring stable isotope values are positively and linearly correlated. In addition, any change in the mother–offspring bulk tissues and individual amino acids that occurred during gestation was investigated. Whiskers sampled from southern elephant seal pups (*Mirounga leonina*) and temporally overlapping whiskers from their mothers were analyzed. This included $n = 1895$ chronologically subsampled whisker segments for bulk tissue δ^{15}N and δ^{13}C in total and $n = 20$ whisker segments for amino acid δ^{15}N values, sampled from recently weaned pups ($n = 17$), juvenile southern elephant seals (SES) < 2 years old ($n = 23$) and adult female SES ($n = 17$), which included nine mother–offspring pairs. In contrast to previous studies, the mother–offspring pairs were not in isotopic equilibrium or linearly correlated during gestation: the Δ^{15}N and Δ^{13}C mother–offspring offsets increased by 0.8 and 1.2‰, respectively, during gestation. The foetal bulk δ^{15}N values were 1.7 ± 0.5‰ (0.9–2.7‰) higher than mothers' δ^{15}N values before birth, while the foetal δ^{13}C increased by ~1.7‰ during gestation and were 1.0 ± 0.5‰ (0.0–1.9‰) higher than their mothers' δ^{13}C at the end of pregnancy. The mother–offspring serine and glycine Δ^{15}N differed by ~4.3‰, while the foetal alanine δ^{15}N values were 1.4‰ lower than that of their mothers during the third trimester of pregnancy. The observed mother–offspring δ^{15}N differences are likely explained by shuttling of glutamate–glutamine and glycine–serine amongst skeletal muscle, liver, placenta and foetal tissue. Foetal development relies primarily on remobilized endogenous maternal proteinaceous sources. Researchers should consider foetal physiology when using offspring bulk tissue isotope values as biomarkers for the mother's isotopic composition as part of monitoring programmes.

Key words: Amino acid–specific stable isotopes, intrauterine, marine mammals, mother–offspring pairs, nutrition, whiskers

Editor: Steven Cooke

Received 25 January 2020; Revised 14 April 2020; Accepted 14 June 2020

Cite as: Lübcker N, Whiteman JP, Newsome SD, Millar RP, de Bruyn PJN (2020) Can the carbon and nitrogen isotope values of offspring be used as a proxy for their mother's diet? Using foetal physiology to interpret bulk tissue and amino acid δ^{15}N values. *Conserv Physiol* 8(1): coaa060; doi:10.1093/conphys/coaa060.

Introduction

The interaction between the nutritional ecology and reproduction of organisms regulates their population dynamics (e.g. Gardner and Grafen, 2009; Bergman *et al.*, 2019). Female fecundity often controls population growth rates (Pistorius *et al.*, 1999; Gardner and Grafen, 2009; Birkhofer *et al.*, 2017), and female fitness is highly correlated with diet composition (McMahon *et al.*, 2000; Donnelly *et al.*, 2003). However, traditional methods for dietary analyses, such as stomach lavage and scat analysis, only provide a 'snapshot' of the most recently ingested prey (Tollit *et al.*, 2007, 2015; McInnes *et al.*, 2016; Roslin and Majaneva, 2016) and are often confounded by varied retention of diagnostic prey remains and an inability to account for spatial and temporal dietary variations. Sampling approaches that can provide longitudinal dietary data are required and are especially insightful for species with complex life histories that include extensive movement between foraging and breeding grounds (Young *et al.*, 2015; Nielsen *et al.*, 2018). However, such approaches must consider that the capture and handling of free-ranging large animals for dietary investigations are notoriously challenging.

Indirect biochemical analyses of non-lethally sampled tissues are increasingly utilized for longitudinal, retrospective studies of animal ecology and physiology (Newsome *et al.*, 2010; Pauli *et al.*, 2010; Trumble *et al.*, 2018). Specifically, the carbon ($\delta^{13}C$) and nitrogen ($\delta^{15}N$) stable isotope values of animal tissues are particularly useful for reconstructing diet composition as well as inferring broad-scale patterns in habitat use and movement (Newsome *et al.*, 2010; Ohkouchi *et al.*, 2017; Pagani-Núñez *et al.*, 2017). $\delta^{13}C$ and $\delta^{15}N$ values of a consumers' tissue(s) reflect its diet but are offset in a predictable fashion due to physiologically mediated processes associated with nutrient assimilation and excretion (DeNiro and Epstein, 1976). For example, isotopically heavier ^{15}N is preferentially retained in the whole-body nitrogen pool because deamination of amino acids tends to remove ^{14}N that is excreted via urine and faeces (DeNiro and Epstein, 1976; Post, 2002). Such diet-to-tissue isotopic offsets ($\Delta^{13}C_{diet-tissue}$ or $\Delta^{15}N_{diet-tissue}$) are commonly called trophic discrimination factors (TDFs) and are required for the use of mixing models to quantify dietary inputs (Parnell *et al.*, 2013).

In comparison to adults, offspring can often be handled more readily and safely (Jenkins *et al.*, 2001) and as such are regularly targeted for isotope analysis (Pagani-Núñez *et al.*, 2017). It is safe to assume that the tissues of offspring sampled shortly after parturition were synthesized *in utero* (intrauterine synthesized tissues; Lowther *et al.*, 2013). Paired mother–offspring stable isotope values of both income and capital breeders are often assumed to be either in isotopic equilibrium or positively correlated (e.g. Jenkins *et al.*, 2001; Table 1 and S1). As such, the isotopic composition of tissue sampled from neonates or nursing offspring are widely used to infer the diet and foraging habitats of their mothers (e.g. Table 1). Shortly after birth, the isotopic values of offspring tissues begin to equilibrate with maternal milk, resulting in increased $\delta^{15}N$ values (~+0.3 – +3.0‰; Fogel, 1989; Newsome *et al.*, 2006; De Luca *et al.*, 2012). Patterns in $\delta^{13}C$ values between nursing offspring and their mothers are more variable and can be either positive or negative depending on the lipid content of maternal milk (Table 1 and S1). Although species-specific mother–offspring isotopic discrimination can occur during both gestation and lactation (Table 1), few studies have considered if or how such discrimination changes as gestation and lactation progress (but see Stricker *et al.*, 2015; Habran *et al.*, 2019). Moreover, studies validating this approach relied on a single, cross-sectional sampling approach focused on offspring that were wholly dependent on maternal milk for their nutrition (Dalerum *et al.*, 2007; Drago *et al.*, 2010; De Luca *et al.*, 2012; but see Hindell *et al.*, 2012; Table S1).

Foetal nutritional demands may change as gestation progresses (Lindsay *et al.*, 2015), and therefore, the assumption that mother–offspring isotopic offsets remain constant throughout pregnancy is unlikely. However, when using continuously growing, metabolically inert keratinous tissues such as whiskers or baleen to chronologically analyze the trophic ecology of mammals, it is assumed that TDFs remain constant during the period (months to years) of tissue synthesis (Lowther and Goldsworthy, 2011; Stricker *et al.*, 2015). To our knowledge, the only measurements available for mother–offspring whisker isotopic offsets are for whiskers of income-breeding pinnipeds, including Australian (*Neophoca cinereal*; Lowther and Goldsworthy, 2011) and Steller (*Eumetopias jubatus*; Stricker *et al.*, 2015) sea lions. For sea lion pup whiskers grown during gestation, studies show negligible differences in $\Delta^{13}C$ between mother and pup, but a slight and significant increase in foetus $\delta^{15}N$ values (~0.8‰) relative to their mothers (Lowther and Goldsworthy, 2011; Stricker *et al.*, 2015). For sea lion pup whiskers grown while nursing, mean mother–offspring $\Delta^{15}N$ increased to ~1.6‰ (Stricker *et al.*, 2015). The $\delta^{15}N$ and $\delta^{13}C$ values of blood sampled from phocid offspring, such as southern elephant seals (SES; *Mirounga leonina*) and northern elephant seals (*M. angustirostris*), have similarly been used to reconstruct the maternal trophic ecology (Ducatez *et al.*, 2008; Habran *et al.*, 2010, 2019). Until now, the possibility that mother–offspring isotopic offsets might change during the 7–9-month gestation period has not been investigated. Coupling isotope analysis of bulk keratin tissues and their constituent amino acids (Whiteman *et al.*, 2019) could provide information on the maternal resource pool that supports foetal development as gestation progresses.

This study evaluates the assumption that bulk tissue $\delta^{13}C$ and $\delta^{15}N$ values measured along the length of phocid pup whiskers grown *in utero* predictably reflect the isotopic composition of their mothers (e.g. Lerner *et al.*, 2018). Variation in $\delta^{13}C$ and $\delta^{15}N$ values of subsampled whiskers collected from recently weaned SES pups (~23-day-old) and juvenile SES (<2-year-old) were used to isolate the por-

Table 1: Differences between the mother–offspring bulk tissue δ^{15}N and δ^{13}C values measured in offspring tissue (whiskers, whole blood, serum/plasma, red blood cells, skin biopsy, hair; studies of fossilized material are excluded) of 31 mammal species in 25 studies to infer the foraging habits of their mothers during gestation and lactation.

Breeding strategy	Period	$\Delta^{15}N_{mother-offspring}$ (‰)	$\Delta^{13}C_{mother-offspring}$ (‰)
Income breeder	Intrauterine/late gestation[d,j,l]	+0.8–+1.5	+0.4–+1.1
	Lactation[a,b,d,g,i,l,n,p,q,r]	+0.8–+3.0	−2.9–+1.2
Capital breeder	Intrauterine/late gestation[e,f,h,k]	+0.5–+2.0	+0.1–+1.1
	Lactation[a,c,f,g,h,k,m,o]	+0.3–+2.6	−1.2–+1.9
Applications			
Trophic ecology reconstructions[o,w]	Foraging ecotypes[a,c,u]	Traced breast feeding or weaning[l,m]	Inter-colony/site variation in maternal foraging habits[b,s,t,v,e,x,y]

[a]Lowther and Goldsworthy, 2011; [b]Porras-Peters *et al.*, 2008; [c]Ducatez *et al.*, 2008; [d]Stricker *et al.*, 2015; [e]Hindell *et al.*, 2012; [f]Borrell *et al.*, 2016; [g]Jenkins *et al.*, 2001; [h]Habran *et al.*, 2010; [i]Dalerum *et al.*, 2007; [j]De Luca *et al.*, 2012; [k]Habran *et al.*, 2019; [l]Fogel *et al.*, 1997; [m]Polischuk *et al.*, 2001; [n]Cherel *et al.*, 2015; [o]Hobson *et al.*, 2000; [p]Elorriaga-Verplancken *et al.*, 2016; [q]Sare *et al.*, 2005; [r]Kravchenko *et al.*, 2019; [s]Wolf *et al.*, 2008; [t]Aurioles *et al.*, 2006; [u]Baylis *et al.*, 2016; [v]Drago *et al.*, 2010, [w]Lerner *et al.*, 2018; [x]Lowther *et al.*, 2013; [y]Scherer *et al.*, 2015. See Table S1 for additional details of studies listed herein.

tions of the whisker grown during gestation, which was compared with similar segments of adult female whiskers to provide isotopic signatures between unpaired mother–offspring samples. Paired mother–offspring whisker samples were used to describe individual and temporal differences in the mother–offspring bulk tissue isotopic discrimination as well as patterns in the δ^{13}C and δ^{15}N values of individual amino acids in the whiskers. Our final objective was to assess changes in longitudinal amino acid isotopic signatures in the endogenous resource pool that supports foetal development. Few studies have analyzed concurrently synthesised tissues from both the mother and offspring (Borrell *et al.*, 2016), and our study represents the first combined bulk tissue and amino acid isotope approach to investigate the resource pool contributing to foetal development, explore foetal amino acid metabolism and provide mechanistic explanations between mother and offspring isotope offsets in SES.

Materials and methods

Study area and whisker collection

Whiskers from recently weaned SES pups ($n = 17$), juveniles ($n = 23$) and adult female SES (>3-year-old; $n = 17$) were cut as close to the skin as possible. All samples were collected from individually identified SESs (flipper tags) on Marion Island (46.7731° S, 37.8525° E) in the Southern Ocean (Pistorius *et al.*, 2011). Sampling procedures and chemical immobilization techniques used on SES are detailed in Lübcker *et al.*, (2017) and Bester (1988).

Pup whisker growth rates

Segments of SES pup whiskers that reflected growth *in utero* were identified. Foetal whiskers of SES are known to be ~10 mm long at 60-day post-conception when blastocyst implantation occurs at the end of the female pelage molt (Ling, 1966). A ~12-mm whisker segment remained after the initial whisker were removed from pups <2 days after weaning during the breeding seasons of October 2009–2014. This embedded whisker segment was grown during the ~21–23-day SES lactation period (Fig. S1; Lübcker *et al.*, 2016). Regrown *ex utero* whisker growth sampled from SES juveniles ($n = 17$) was used to identify the lactation period. These whisker 'regrowths' were 68.7 ± 13.8 mm long and were collected during the annual molt in January 2013 and 2014 (Lübcker *et al.*, 2016). Isotope values of whisker regrowths and (previously unsampled) fully grown whiskers collected from juvenile SES (<2 years old; $n = 6$; 102.0 ± 26.8 mm long) collected after these individual SES spent a year at sea (Fig. S2) were used to confirm that no portion of the whiskers grown *ex utero* was included when assessing the *in utero* mother–offspring whisker isotopic offsets.

Identifying segments of adult female whiskers reflecting gestation

Isolating the adult SES female whisker segments reflecting gestation, and subsequently aligning these segments with the foetal (intrauterine) whisker growth, requires detailed information about the adult female whisker growth rate and history (e.g. McHuron *et al.*, 2019). The segments of the adult female whiskers grown on land while fasting can be identified based on the chronology of both bulk tissue and amino acid δ^{15}N values (McHuron *et al.*, 2019; Lübcker *et al.*, 2020). The fasting-enriched δ^{15}N values of adult female whiskers start declining at the onset of the post-molt foraging period, which were assumed to overlap with the delayed blastocyst implantation that occurs during the molt, although the timing of blastocyst implantation can be variable (Ling, 2013; McHuron *et al.*, 2019; Lübcker *et al.*, 2020). The whisker segments of the same $n = 17$ breeding adult females

that reflected gestation were contrasted to isotope values of unpaired, *in utero* grown pup whiskers.

The amino acid $\delta^{15}N$ values measured in whiskers sampled from five recently weaned SES pups were compared to temporally matched amino acid $\delta^{15}N$ values measured in the whiskers of their mothers (Lübcker *et al.*, 2020). From these five SES mothers, we analyzed two segments per whisker that were grown during the first/second trimester of pregnancy (middle of whisker: T1/2-mother) and the third trimester (base of whisker: T3-mother; $n = 10$ samples; Fig. S1). The maternal amino acid $\delta^{15}N$ values measured during T1/2 and T3 were compared to the temporally overlapping *in utero* grown whiskers sampled from their offspring ($n = 5$ pairs; detailed below).

Paired mother–offspring whisker sampling

Whiskers collected from recently weaned SES pups ($n = 5$) were subdivided into two segments per whisker to obtain the required sample mass (~8 mg) needed for amino acid $\delta^{15}N$ and $\delta^{13}C$ analysis; this sampling strategy produced 10 total samples that were categorized as either from the tip (T1/2-foetus) or base (T3-foetus) of the whisker (Fig. S1). The distal T1/2-foetus segment was grown during the first and second trimesters of pregnancy while the basal T3-foetus segment reflected the third trimester of pregnancy (Table 2). The position along the length of the maternal whiskers where the overlapping foetal whisker growth would have started was then identified (Supplementary Material). Furthermore, to ensure that the bulk tissue isotope data are temporally comparable to the amino acid $\delta^{15}N$ data and that the maternal and foetal isotope data overlapped; the first-to-second trimester (T1/2-mother) and third-trimester (T3-mother) bulk tissue isotope data of adult females were pooled (Fig. S1). Similarly, the bulk tissue isotope data of each recently weaned SES pup that reflect the time periods represented by T1/2-foetus and T3-foetus were pooled to correspond to the time periods for which accompanying amino acid $\delta^{15}N$ data were available (Fig. 2). Grouping data into two time points (T1/2 and T3) reduced the risk that autocorrelation influenced the statistical comparisons and that any temporal mismatching of the mother–offspring isotope data could affect our conclusions. The difference in the mother–offspring stable isotope values was reported as the mean difference ($\Delta^{15}N$ or $\Delta^{13}C$) for each time point.

Bulk tissue $\delta^{15}N$ and $\delta^{13}C$ tissue values representing SES foetal growth were compared with their mother's isotopes during the same time period ($n = 4$ pairs). All paired mother–offspring samples, which included four pairs for bulk tissue analysis and five pairs for amino acid analysis, were collected during the 2015 breeding season. The logistical coordination and associated risk involved with the temporary marking of unweaned pups (De Bruyn *et al.*, 2008) and subsequent sampling of mother–offspring pairs when the pups are weaned before the mothers return to sea, restricted our sample size of mother–offspring pairs (Stricker *et al.*, 2015).

Bulk tissue- and amino acid stable isotope analysis

For bulk tissue isotope analysis, all whiskers were chronologically sectioned into 2.0 ± 0.4 mm sections, and surficial contaminants were removed by rinsing in a (2:1) chloroform:methanol solvent solution (Lübcker *et al.*, 2017). A ~0.5-mg aliquot of each whisker segment was weighed into a tin capsule and measured $\delta^{13}C$ and $\delta^{15}N$ values using a Thermo Scientific Flash 1112 Series Elemental Analyzer (Thermo^{TM}, Thermo Fisher Scientific, Bremen, Germany) coupled to a Thermo Scientific Delta V Plus isotope ratio mass spectrometer (EA-IRMS; Thermo Finnigan, Bremen, Germany) at the Stable Isotope Laboratory at the University of Pretoria (Pretoria, South Africa). The thinner distal portion of the whiskers required larger sections to obtain the required sample mass for $\delta^{13}C$ and $\delta^{15}N$ analysis. Isotopic measurements were corrected to the international reference standards, Vienna Pee Dee Belemnite (VPDB) for $\delta^{13}C$ and atmospheric air for $\delta^{15}N$. In each run, two internal reference materials (Merck gel and DL-alanine) were used to assess analytical precision. The results are expressed in parts per mil (‰) relative to the international standard atmospheric N_2. Sample precision (SD) was ±0.3‰ for $\delta^{15}N$ and ± 0.2‰ for $\delta^{13}C$.

For amino acid $\delta^{15}N$ analysis, pup whisker segments with a mean (± SD) sample mass of 8.2 ± 2.0 mg (minimum: 5.6 mg; $n = 10$ samples) and adult female whisker segments with a mass of 9.9 ± 2.9 mg ($n = 30$ samples) were hydrolyzed in 1 ml 6 N hydrochloric acid (HCl) for 20 h at 110°C in muffled glassware. The SES whisker segment amino acids were hydrolyzed using 2-isopropanol and *N*-TFAA (Fantle *et al.*, 1999). The analyses were performed using a 60 m DB-5 column (SGE Analytical Science) in a Thermo Scientific Trace 1310 gas chromatographer coupled to a Isolink II and Thermo Scientific Delta V Plus IRMS at the University of New Mexico Center for Stable Isotopes (Albuquerque, NM, USA). This method provided $\delta^{15}N$ measurement of 13 amino acids: alanine (Ala), isoleucine (Iso), leucine (Leu), valine (Val), proline (Pro), glycine (Gly), serine (Ser), phenylalanine (Phe), lysine (Lys), tyrosine (Tyr), threonine (Thr), glutamic acid (Glu) and aspartic acid (Asp). The within-run precision (SD) for amino acid $\delta^{15}N$ analysis for multiple injections of duplicate unknown samples averaged 0.3‰ and ranged from 0.3‰ for Lys and 0.4‰ for Ile. The precision of the stock internal stock standard consisting of pure amino acids (Sigma–Aldrich Co.) that bracketed each set of unknown samples averaged 0.6‰ and ranged from 0.4‰ for Thr and 0.8‰ for Tyr.

Statistical analyses

A piecewise linear regression model was applied to characterize isotopic variation along the length of the whisker that corresponds to specific life-history events, using the package *segmented* (Muggeo, 2008) in R (version 3.4.4). Breakpoints in the bulk tissue $\delta^{15}N$ and $\delta^{13}C$ values were estimated by visual inspection of the plotted data and the fitted Loess

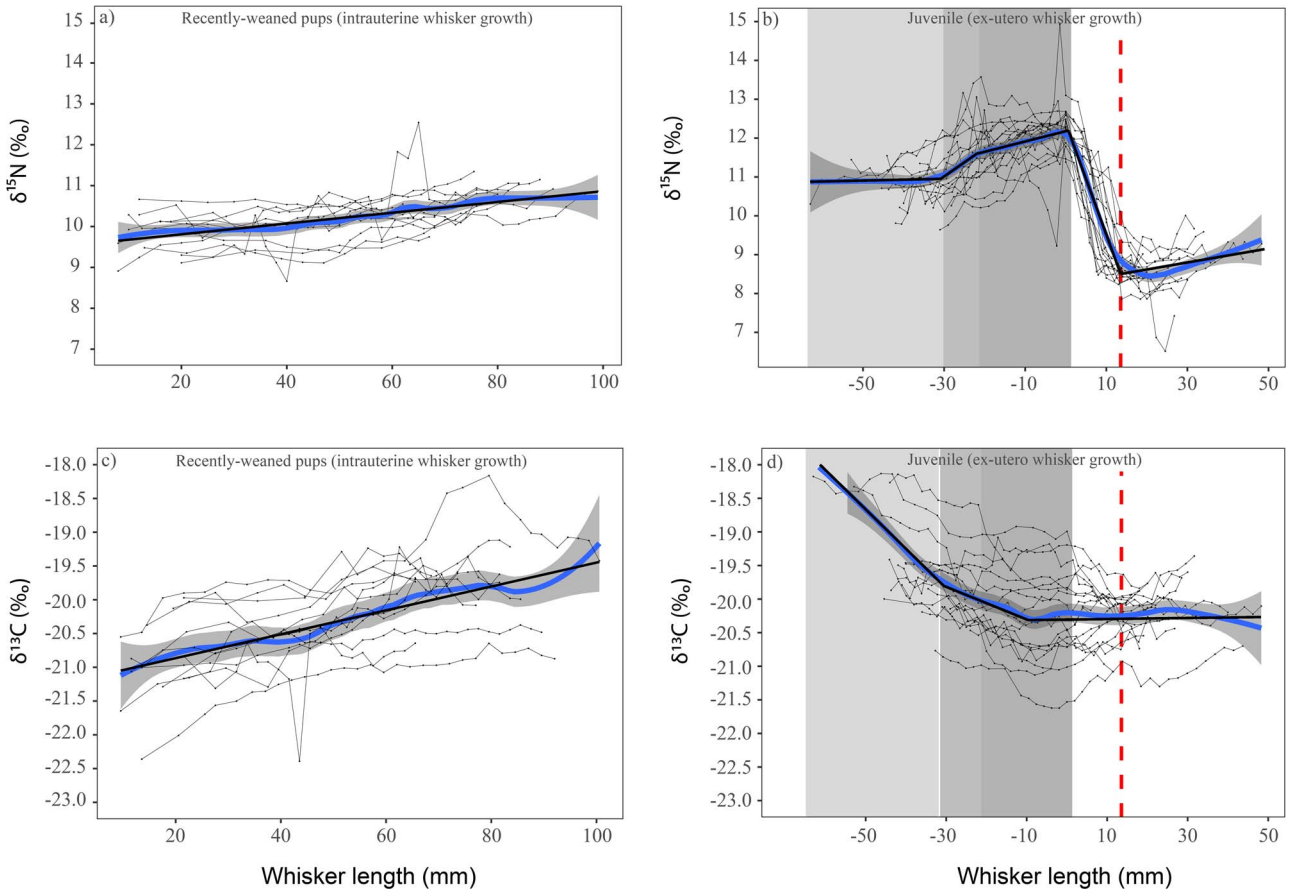

Figure 1: Chronology of corresponding bulk tissue δ^{15}N (**a**, **b**) and δ^{13}C values (**c**, **d**) measured along the length of intrauterine grown whiskers sampled from recently weaned pups (a, c), and (b, d) *ex utero* grown whisker regrowths of $n = 17$ juvenile southern elephant seals (*Mirounga leonina*), fitted with a linear regression (black line) and a Loess smoother (SE in grey = 0.12‰, blue line). The growth starts from the onset of gestation (left) ending just before birth. The plot position (*x* axis) was set to zero based on the beginning of the post-weaning δ^{15}N depletion (b, d), with light grey (far left) reflecting the intrauterine grown segment of the whiskers, followed by lactation and the post-weaning fast depicted in darker grey (right). The red vertical line indicates the start of the predicted independent foraging.

smoothing polynomial regression. A least trimmed squares robust regression model (*ltsReg* package in R) was applied to describe the correlation of maternal and foetal bulk tissue isotope data over the whisker length, respectively. A similar approach was used to characterize the correlation of the mother–offspring isotopic differences for each pair (Table S4). Lastly, linear mixed-effect models (*lme4* package in R 1.1–21; Bates *et al*. 2015) were used to assess the influence of maternal whisker bulk isotope values on the temporally paired offspring whisker values. In these models, the stable isotope value of offspring whisker (e.g. $\delta^{15}N_{offspring}$) was predicted by the fixed effect of the corresponding value from the mother (e.g. $\delta^{15}N_{mother}$) and the random effects of *period* (i.e. T1/2-foetus or T3-foetus) and *pairs* (*pair* 1–4). These mixed-effect models included data from 67 paired mother–offspring whisker segments (39 from T1/2-foetus, 28 from T3-foetus). The inclusion of *pairs* and *period* as random effects accounted for non-independence of repeated measures between the mother and offspring. Where applicable, residual and data normalities were assessed using a Shapiro–Wilk test. Visual inspection of residual plots then confirmed homoscedasticity and normality. The *P*-values of the full model were ascertained via restricted likelihood ratio tests and calculated based on Satterthwaite's approximations (Luke, 2017) by comparison with reduced models that excluded the random effects (e.g. Grecian *et al*., 2015) using the *lmerTest* package in R (Kuznetsova *et al*. 2017; version 3.1–1). Model selection was based on Akaike's information criterion (*AIC*) and Bayesian Information Criterion (*BIC*) values (Burnham and Anderson, 2002). The proportion variance explained by the final models is expressed as marginal and conditional R^2 values ($R^2_{GLMM(m)}$ *and* $R^2_{GLMM(c)}$; Nakagawa and Schielzeth, 2013). The error (residual) term (ϵ) in the models can be attributed to intra-individual variability in δ^{13}C and δ^{15}N (Hückstädt *et al*., 2012). For bulk tissue δ^{15}N, the mean and standard deviation (SD) are reported, while the medians and associated upper and lower 95% confidence intervals are reported for the amino acid δ^{15}N results. The mean difference between

Table 2: Bulk tissue δ^{15}N and δ^{13}C values (Mean ± SD) reflecting different life-history events captured along the length of whiskers sampled for recently weaned pups, juvenile and breeding adult female southern elephant seals (*Mirounga leonina*), corresponding to the first-to-second trimester of gestation (T1/2) and the third trimester of pregnancy (T3).

Age class	Sample size (number of individuals)	Period	Whisker/segment length (mm)	Number of segments (average/individual)	δ^{15}N (‰)	δ^{13}C (‰)
Recently weaned pups	12	**Full intrauterine**	**78.4 ± 8.3**	**252 (21.0 ± 6.0)**	**10.2 ± 0.5**	**−20.3 ± 0.7**
		T1/2-foetus	35.0 ± 4.2	110	10.0 ± 0.5	−20.6 ± 0.6
		T3-foetus	13.4 ± 5.7	76	10.5 ± 0.5	−19.9 ± 0.6
Juveniles	17	**Full regrowth**	**68.7 ± 13.8**	**560 (32.9 ± 6.6)**	-	-
		Intrauterine	10.0 ± 8.2	77	10.9 ± 0.5	−19.3 ± 0.7
		Lactation	6.6 ± 1.4	73	11.3 ± 0.8	−19.9 ± 0.6
		Transition	10.3 ± 0.8	105	-	-
		Fasting	20.5 ± 1.1	186	11.9 ± 0.7	−20.2 ± 0.6
		Foraging	13.4 ± 9.8	119	8.7 ± 0.5	−20.2 ± 0.4
Adult females	17	**Full whisker**	**116.4 ± 19.1**	**805*** **(47.4 ± 10.0)**	**-**	**-**
		Fasting[a]	21.4 ± 12.1	136	-	−19.4 ± 0.9
		Fasting[b]	11.5 ± 1.3	108	11.6 ± 0.8†	−19.2 ± 0.8
		Transition	25.6 ± 1.3	231	11.2 ± 0.8†	−19.6 ± 0.9
		Gestation	40.1 ± 19.5	330	10.0 ± 0.7†	−20.0 ± 1.1
		T1/2-mother	35.1 ± 7.1	309	10.1 ± 0.6	−20.1 ± 1.0
		T3-mother	10.5 ± 6.2	68	9.6 ± 0.8	−20.3 ± 1.2

*Excludes $n = 16$ plucked whisker segments. Mean (± SD) attributes of full whiskers are given in bold.
†Values correspond to piecewise regression of nitrogen isotope values, as reported in Lübcker *et al.*, (2020).
- = Not applicable.
[a,b]Breakpoint during foraging.

the offspring's amino acid δ^{15}N values and its mother's Phe ($\Delta^{15}N_{Pup\text{-}MotherPhe}$) and Lys ($\Delta^{15}N_{Pup\text{-}MotherLys}$) δ^{15}N value for each pair were calculated. Phe and Lys are source amino acids and their δ^{15}N values reflect the nitrogen isotope composition of primary producers at the base of the food web (O'Connell, 2017) and therefore used to assess potential baseline isotopic variability when comparing amino acid δ^{15}N data amongst individuals.

Results

Juvenile SES whisker bulk tissue δ^{15}N and δ^{13}C values

Bulk tissue δ^{15}N values measured along the length of whiskers sampled from both recently weaned pups (Fig. 1a) and juvenile SES (Fig. 1b) increased significantly (Kruskal–Wallis $\chi^2 = 351.75$, df = 4, $P < 0.001$) from the onset of gestation to the end of the post-weaning fast (also see Fig. S2). The lactation-associated δ^{15}N values (Fig. S1) of the ∼12-mm whisker segment left embedded in the muzzle of recently weaned pups had significantly higher δ^{15}N values by ∼0.7‰ than pre-parturition δ^{15}N values in the distal 12 mm of the resulting whisker regrowths Table 2; Fig. 1b). It was confirmed that the entire whisker sampled from recently weaned pups only reflects whisker growth that occurred *in utero* and does not include post-parturition growth influenced by nursing. δ^{15}N values increased by ∼1.0‰ during gestation as measured along the length of the whiskers sampled from $n = 12$ recently weaned SES pups (least-squared linear regression; $y = 0.013 \times + 9.6$, SE = 0.4‰; df = 242; *Adj.* $R^2 = 0.32$; $P < 0.001$; Fig. 1a).

The corresponding δ^{13}C values measured along the length of intrauterine grown whiskers sampled from recently weaned pups increased by ∼1.7‰ as gestation progressed (Fig. 1c; least-squared linear regression: SE = 0.5‰; df = 244; *Adj.* $R^2 = 0.40$; $P < 0.001$). δ^{13}C values then declined by ∼0.6‰ during lactation relative to pre-parturition values (Kruskal–Wallis $\chi^2 = 102.86$, df = 4, $P < 0.001$; Fig. 1d) and decreased by a further 0.3‰ during the post-weaning fast (piecewise linear regression: SE = 0.6‰; df = 554; *Adj.* $R^2 = 0.29$; $P < 0.001$; Table S2).

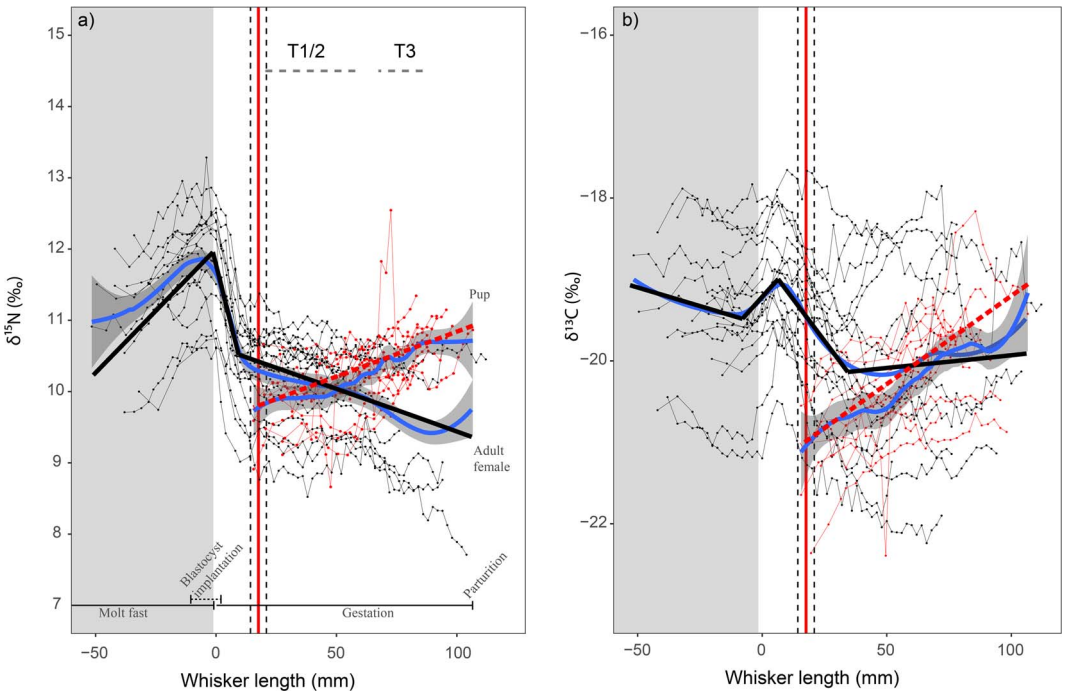

Figure 2: Temporally overlapping bulk tissue δ^{15}N (**a**) and δ^{13}C (**b**) values measured chronologically along the length of whiskers sampled from unpaired adult female ($n = 17$), and intrauterine grown whiskers sampled from $n = 12$ recently weaned southern elephant seal pups (*Mirounga leonina*). The plot position (x axis) was set to zero based on the onset of the post-molt fast-associated δ^{15}N depletion, with grey reflecting the segments of the adult female whiskers predicted to have grown on land. The solid red vertical line indicates the position along the adult female whiskers where the foetal (intrauterine) whisker growth started with the standard deviation indicated by the vertical dashed lines. The whisker segments were divided into two periods corresponding to the first-to-second trimester of gestation (T1/2) and the third trimester of pregnancy (T3) for further analyses. The blue line with grey bars represents the fitted Loess smoother (span = 0.3), while the piecewise linear regression model is indicated by black lines. Least trimmed squares robust regression models were used to illustrate the correlation of the foetal isotope values (red dashed lines).

Adult female whisker bulk tissue δ^{15}N and δ^{13}C values

The increase of the bulk whisker δ^{15}N values of ~1.8‰ measured in the distal segments of adult female whiskers are likely associated with fasting (piecewise linear regression: SE = 0.7‰; df = 799; *Adj.* $R^2 = 0.48$; $P < 0.001$; Fig. 2a), and coupled with the subsequent precipitous decrease of 1.4‰ over the length of their whiskers associated with the post-molt foraging trip, enabled identification of the switch from endogenous to exogenous resource use (Table 2). After this initial steep decline, δ^{15}N values continued to decrease by on average ~1.3‰ over the length of their whiskers and reflect at sea foraging during which females are pregnant ($P < 0.001$; $\delta^{15}\text{N} = -0.012 \times + 10.6$).

Bulk tissue δ^{13}C values (Fig. 2b) for adult females differed significantly along whiskers (Kruskal–Wallis $\chi^2 = 64.8$, df = 3, $P < 0.001$), and observed changes were associated with life-history events (piecewise linear regression SE = 1.0‰; df = 813; *Adj.* $R^2 = 0.12$; $P < 0.001$). δ^{13}C values in whisker segments grown while fasting during the molt were significantly higher by ~0.8‰ in comparison to portions of the whisker grown during the post-molting foraging trip ($P < 0.001$; Table 2 and S2). Inter-individual variation in δ^{13}C values (SD: 1.0–1.2‰; Table 2) occurred in the portion of the whisker grown during the post-molting foraging trip (Fig. 2b; S3–S4).

Overlapping adult female and foetal whisker bulk tissue δ^{15}N and δ^{13}C values

Adult female and foetal whisker growth overlap started 56.0 ± 7.0 mm from the tip of female whiskers based on whisker growth rates and the δ^{15}N depletion associated with the onset of active foraging detected along the whiskers of 17 adult females (Fig. 2a, Supplementary Material). The slope of the increase in foetal δ^{15}N (0.013‰/mm) was comparable to the slope of the decline in adult female δ^{15}N (−0.012‰/mm), and on average female δ^{15}N values declined by ~0.5‰ while foetal δ^{15}N increased by ~0.5‰ throughout pregnancy (Fig. 2a). The pooled (unpaired) mother–offspring bulk whisker isotope data were grouped into two overlapping time points corresponding to the approach used to generate our amino acid dataset (T1/2, T3; Fig. 2a; Table 2). The

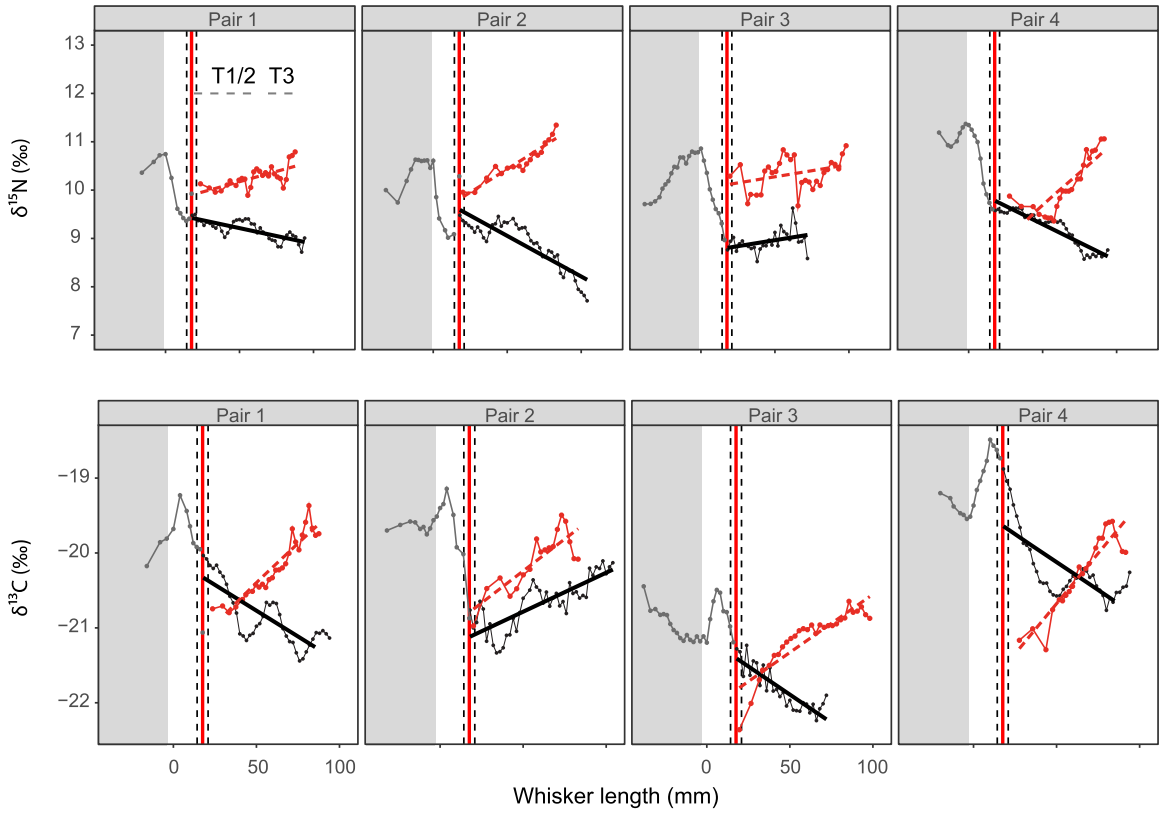

Figure 3: Bulk tissue $\delta^{15}N$ and $\delta^{13}C$ values measured sequentially along the length of whiskers sampled from four southern elephant seal (SES, *Mirounga leonina*) mother–offspring pairs. The predicted onset of the overlap between the foetal and maternal whisker growth is indicated by the vertical red line (SE ± 3.3 mm, black dashed lines). The segments of the whisker grown on land while fasting is indicated in grey. Overlapping sampled whisker growth segments T1/2 and T3 are indicated in the top left panel. The least trimmed squares robust regression models used to illustrate the correlation of the maternal and foetal isotope values, respectively (red dashed line), are detailed elsewhere (Table S2).

bulk whisker $\delta^{15}N$ and $\delta^{13}C$ values differed significantly between T1/2 and T3 ($\delta^{15}N$: Kruskal–Wallis $\chi^2 = 64.1$, df = 3, $P < 0.001$; $\delta^{13}C$: Kruskal–Wallis $\chi^2 = 46.3$, df = 3, $P < 0.001$).

Paired mother–offspring bulk tissue $\delta^{15}N$ and $\delta^{13}C$ values

Most of the paired maternal ($n = 149$ whisker segments) and offspring ($n = 97$ whisker segments) $\delta^{15}N$ and $\delta^{13}C$ values were significantly negatively correlated ($P < 0.001$; least trimmed squares robust regression models, Table S3); the exception was $\delta^{15}N$ values for Pair 3 ($P = 0.07$; Fig. 3). Excluding Pair 3, the median adjusted R^2 values for the relationships between mother and foetal $\delta^{15}N$ and $\delta^{13}C$ values were 0.8 ± 0.1 and 0.8 ± 0.1 (± SE) respectively, indicating strong linear negative correlation as gestation progressed (Table S3). The mean bulk whisker $\delta^{15}N$ and $\delta^{13}C$ values of mother–offspring pairs differed significantly (Kruskal–Wallis $\chi^2 = 46.3$, df = 3, $P < 0.001$), except for the $\delta^{13}C$ values of Pair 4 ($P = 1.000$; but see Fig. 3).

The mother–offspring $\Delta^{15}N$ and $\Delta^{13}C$ values of the overlapping 67 whisker segments during T1/2 and T3 increased on average by 0.8 and 1.2‰ respectively, from sampling period T1/2 to T3; T1/2 ($\Delta^{15}N_{mother-offspring}$: 0.9 ± 0.5‰; range: 0.0–1.7‰; T3 $\Delta^{15}N_{mother-offspring}$: 1.7 ± 0.5‰; range: 0.9–2.7‰; T1/2 $\Delta^{13}C_{mother-offspring}$: -0.2 ± 0.6‰; range: −1.6–1.1‰; T3$\Delta^{13}C_{mother-offspring}$:T31.0 ± 0.5‰; range: 0.0–1.9‰). $\Delta^{13}C_{mother-offspring}$ ranged from being −1.6‰ to +1.9‰ before parturition. The least trimmed squares robust regression models describing the temporally matched mother–offspring isotopic correlations are detailed in Table S4 and were all significantly and negatively correlated, except for the $\Delta^{15}N_{mother-offspring}$ values of Pair 1 ($P = 0.62$). Overall, the isotopic composition of mothers and offspring did not appear to be in isotopic equilibrium during gestation (Fig. 4a and b). Based on the three linear mixed-effect model used to describe the influence of the sampling period (T1/2 and T3) and individual pairs (Table S5), the model containing the random effects, *pair* and *period*, described the $\Delta^{15}N_{mother-offspring}$ ($\chi^2 = 13.07$, df = 5, $P < 0.001$, $R^2_{GLMM(c)} = 55.0$) and $\Delta^{13}C_{mother-offspring}$ ($\chi^2 = 52.45$, df = 5, $P < 0.001$, $R^2_{GLMM(c)} = 92.6\%$) relationship the best (Table 3), which is confirmed based on the model *AIC* and *BIC* values (Table S5). For $\Delta^{13}C_{mother-offspring}$,

both random effects significantly affected the model (log-likelihood ratio test; $P < 0.001$). For $\Delta^{15}N_{mother-offspring}$, the sample *pair* had a significant influence on the offspring $\delta^{15}N$ values ($P < 0.001$), while the influence of the sampling *period* were marginal ($P = 0.059$). The maternal $\delta^{15}N$ values were 0.6 ± 0.2‰ (SE; 95% CI: -0.9 – -0.2‰) lower than their offspring's $\delta^{15}N$ values and significantly negatively correlated ($P < 0.01$; Table S6). The maternal $\delta^{13}C$ values were 0.4 ± 0.1‰ (SE; 95% CI: -0.6 – -0.2‰) lower than their offsprings' $\delta^{13}C$ values and were also significantly negatively correlated ($P < 0.001$;Table S7).

Paired mother–offspring amino acid $\delta^{15}N$ values

Apart from Ala (and to a lesser extent Val), $\delta^{15}N$ values of trophic and source amino acids were similar between paired offspring and mothers at T1/2 and T3 (Table S8; Fig. S5). Both Gly and Ser were significantly higher in offspring relative to the median of their mothers by ~4.3‰ (Gly: Kruskal–Wallis $\chi^2 = 14.6$, df = 3, $P < 0.01$; Ser: Kruskal–Wallis $\chi^2 = 13.7$, df = 3, $P < 0.01$; Fig. 5). During T3, Ala $\delta^{15}N$ values in offspring were 1.4‰ lower than the median of their mothers', while Val $\delta^{15}N$ values in offspring were 1.4‰ higher than their mothers' median Val $\delta^{15}N$ values.

Discussion

Contrary to the assumptions made by previous studies, temporally overlapping bulk tissue $\delta^{15}N$ and $\delta^{13}C$ values from paired adult SES females and their offspring, are not in isotopic equilibrium during gestation. Furthermore, offsets in both bulk nitrogen ($\Delta^{15}N$) and carbon ($\Delta^{13}C$) isotope values between mothers and their offspring changed as gestation progressed and were pair specific. The findings of studies that assumed that mother–offspring isotopic offsets remain (i) constant over time and (ii) constant between all sampled pups, or (iii) those that applied no mother–offspring isotopic corrections, should be reconsidered (Table 1 & S1). Our findings shed new light on foetal amino acid metabolism and highlight the mechanisms behind the offsets in mother–offspring bulk tissue $\delta^{15}N$ and $\delta^{13}C$ values observed here and elsewhere (Stricker *et al.*, 2015; Borrell *et al.*, 2016). Ecologists must differentiate between ecological and physiological factors that influence tissue isotope values before drawing inferences about foraging and movement ecology of animals.

Differences in mother–offspring bulk whisker $\delta^{15}N$ and $\delta^{13}C$ values

The $\delta^{15}N$ and $\delta^{13}C$ values measured in tissues sampled from offspring are an attractive proxy for the isotopic composition of their mothers because pup tissues are generally easier to collect than those from adult females (Table 1). While phocids are capital breeders, they do actively forage while pregnant and minimal isotopic differences between mother and foetus are expected, a pattern also observed in income breeders (Table 1 and S1). By extension, most studies assume that mother–offspring $\delta^{15}N$ and $\delta^{13}C$ values are linearly and positively correlated (Jenkins *et al.*, 2001; Table 1), and isotopic discrimination between mother and offspring for carbon ($\Delta^{13}C$) is generally smaller than for nitrogen ($\Delta^{15}N$) (Jenkins *et al.*, 2001; Hindell *et al.*, 2012). It is also assumed that $\Delta^{13}C$ and $\Delta^{15}N$ between income or capital breeding mother–offspring pairs are constant during gestation and consistent amongst individuals (Aurioles *et al.*, 2006; Drago *et al.*, 2010; Hindell *et al.*, 2012; but see Table 1). In contrast to these assumptions and findings, temporally comparable whiskers sampled from SES mothers and their foetuses differ significantly in both $\delta^{15}N$ and $\delta^{13}C$ composition and are not predictably correlated. In 75% of the cases, both $\delta^{15}N$ and $\delta^{13}C$ values of SES mothers and their pups were negatively correlated during gestation (Figs 2–3; this study). While mother–offspring $\Delta^{15}N$ and $\Delta^{13}C$ were generally positive during the third trimester of pregnancy (T3), the magnitude of the offset varied by several per mil amongst pairs. Importantly, SES mother–offspring discrimination changed as gestation progressed (Fig. 3) as both foetal $\delta^{15}N$ and $\delta^{13}C$ values increased relative to the decreasing $\delta^{15}N$ and $\delta^{13}C$ values of their mothers (Fig. 3), which was also observed in the larger dataset for unrelated adult females and pups (Fig. 2). In the only other study to our knowledge that measured paired tissues of phocid mother and pups, the $\delta^{15}N$ values measured in the *in utero* grown whiskers of bearded seal (*Erignathus barbatus*) pups similarly increased consistently from the distal (oldest) to basal (most recent) sections (Hindell *et al.*, 2012).

Foetal $\delta^{15}N$ and $\delta^{13}C$ values were comparable to their mothers in the first and second trimester, but mean $\Delta^{15}N$ and $\Delta^{13}C$ offsets between mother and pup increased to $+1.7 \pm 0.5$ and $+1.0 \pm 0.5$‰, respectively during the third trimester (T3) of pregnancy (Fig. 3). Since whiskers are assumed to be in isotopic equilibrium with blood plasma (Hirons *et al.*, 2001; Newsome *et al.*, 2010), changes in foetal bulk whisker $\delta^{15}N$ and $\delta^{13}C$ values suggest possible differential isotopic discrimination and/or routing of particular amino acids occurred across the placental barrier during pregnancy. Of particular interest is that the negative correlations between pup and mother $\delta^{13}C$ and $\delta^{15}N$ values over the course of gestation were pair-specific and influenced by the period represented (Table 3). This likely reflects differences in the amount of endogenous (stored) maternal protein and adipose fat catabolized to support foetal development and may be related to the maternal body condition as gestation progressed (e.g. Fuller *et al.*, 2004; De Luca *et al.*, 2012). These biochemical mechanisms were further explored via amino acid $\delta^{15}N$ and bulk tissue $\delta^{13}C$ analysis.

Differences in paired mother–offspring amino acid $\delta^{15}N$ values

Interestingly, when corrected for baseline effects by using the mother's lysine and phenylalanine $\delta^{15}N$ values of each mother-

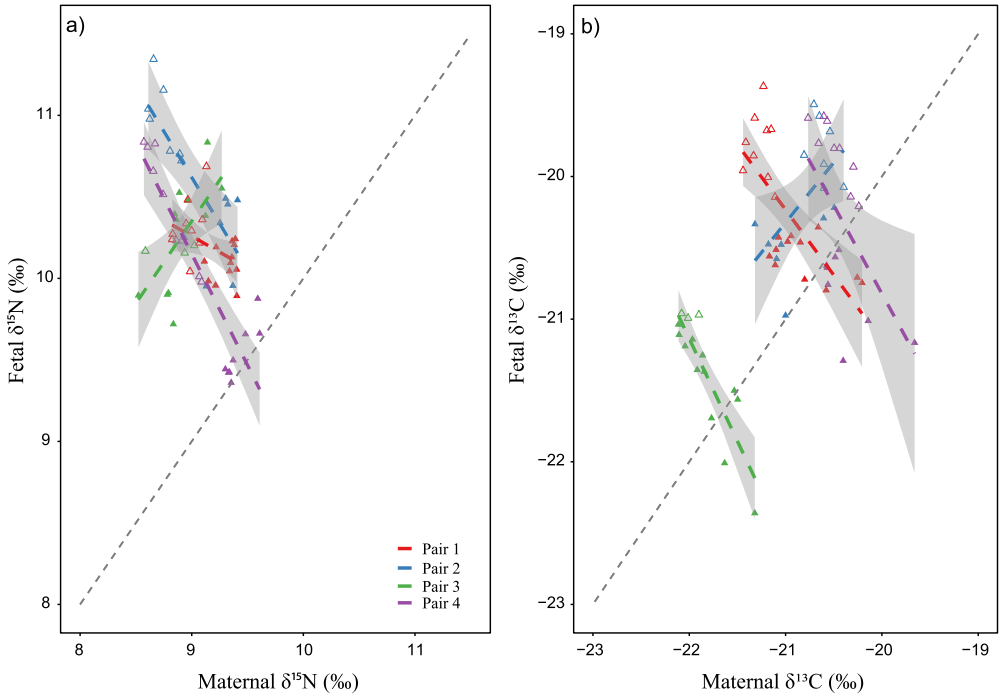

Figure 4: Correlation between maternal and foetal bulk tissue $\delta^{15}N$ (**a**) and $\delta^{13}C$ (**b**) values measured sequentially along the length of whiskers during the first-to-second trimester of gestation (T1/2; solid fill symbols) and third trimester of pregnancy (T3; open symbols) of four southern elephant seal (*Mirounga leonina*) mother–offspring pairs. The dashed black line represents a 1:1 correlation and coloured dashed line represent fitted Loess smoothers for each mother–offspring pair. Details of fitted models are provided elsewhere (Table 3 and S3–S7).

Table 3: Results of the best-fit linear mixed-effect model fit by reduced maximum likelihood (REML, model M_3-$\delta^{15}N/\delta^{13}C$ Table S5) for predicting whisker $\delta^{15}N/\delta^{13}C_{offspring}$ values from their temporally overlapping mother whisker $\delta^{15}N$ values ($\delta^{15}N/\delta^{13}C_{mother}$), with 'period' and 'pair' as random effects.

Model	**M_3-$\delta^{15}N$**			**M_3-$\delta^{13}C$**		
	$\delta^{15}N_{offspring}$			$\delta^{13}C_{offspring}$		
Predictors	Estimates	CI	*P*	Estimates	CI	*P*
(Intercept)	15.06	11.62–18.50	<**0.001**	−28.50	−33.13 – −23.87	<**0.001**
$\delta^{15}N_{mother}$	−0.53	−0.91 – −0.15	**0.007**	−0.38	−0.60 – −0.17	<**0.001**
Random effects						
σ^2	0.08			0.06		
τ_{00}	0.05_{pairs}			0.47_{pairs}		
	0.03_{period}			0.26_{period}		
ICC	0.49			0.92		
n	2_{period}			2_{period}		
	4_{pairs}			4_{pairs}		
Observations	67			67		
Marginal R^2/Conditional R^2	0.116/0.550			0.059/0.926		

Residual variance = σ^2; random intercept variance, or 'between-subject' variance = τ_{00}, intraclass-correlation coefficient = ICC; number of classes/groups = *n*.

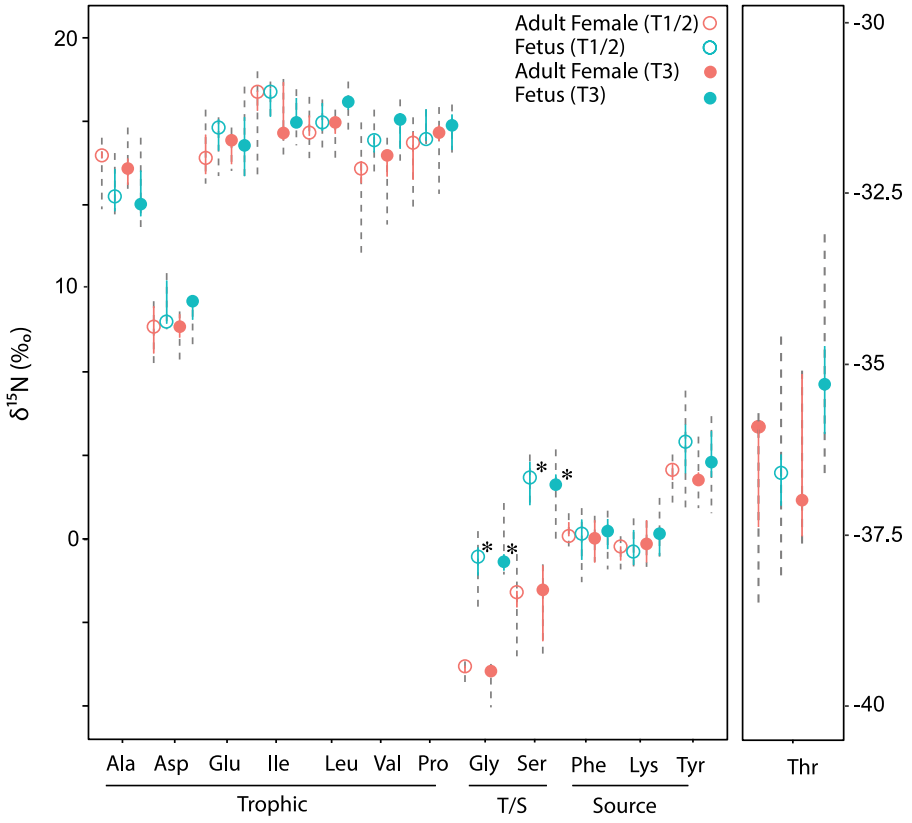

Figure 5: Maternal phenylalanine and lysine δ^{15}N (baseline) corrected amino acid–specific δ^{15}N values measured during the first-to-second trimester of gestation (T1/2; open symbols) and third trimester of pregnancy (T3; closed symbols) along the length of whiskers sampled from five mother–offspring pairs. Adult females (red); intrauterine offspring whisker (blue). T/S = trophic or source amino acid. *$P < 0.05$.

pup pair, most offsets in amino acid δ^{15}N values between mothers and pups were isotopically indistinguishable. Lysine and phenylalanine are thus likely routed from the maternal plasma to the foetus with minimal isotopic alteration. Exceptions were foetal valine and leucine δ^{15}N values, which were ~1.4 and ~0.8‰ higher than that of their mothers, respectively. Likewise, foetal serine and glycine δ^{15}N values were >4‰ higher than that of their mothers (Fig. 5). Given the amino acid composition of α-keratin, which is primarily composed of half-cystine (13.1%), glutamic acid (11.1%), serine (10.8%) and glycine (8.6%) (Marshall *et al.*, 1991), the combined isotopic offsets of glycine and serine can explain the majority of the observed offsets in bulk tissue δ^{15}N values between pups and their mothers (Fig. 2). The glutamate–glutamine and glycine–serine shuttles are likely the most dominant pathways in maternal-foetal amino acid transport (Kalhan, 1998; Fig. 6) and provide a mechanistic explanation for the observed mother–offspring δ^{15}N differences in valine, leucine, glycine, and serine.

Branched-chain amino acids (valine and leucine) are deaminated by the placenta to form glutamate, which is then transaminated to form glutamine and ultimately transferred to the foetus by the glutamate–glutamine shuttle between the mother and foetus (Fig. 6). Amine groups containing ^{14}N are preferentially removed during deamination, resulting in ^{15}N-enrichment of the remaining pool of branch-chained amino acids. This isotopic fractionation may explain the +1.4 and +0.8‰ increase in foetal valine and leucine δ^{15}N values relative to maternal values during the third trimester (T3) of pregnancy. Furthermore, the abundance of glutamate/mine (Wu *et al.*, 2015), along with the rapid rate of cycling of these two amino acids between the mother and foetus, likely eliminates any isotopic discrimination in glutamic acid δ^{15}N values between mother and foetus (Fig. 6): note that the derivatization method used converts both glutamate and glutamine into glutamic acid (Silfer *et al.*, 1991; Whiteman *et al.*, 2019).

The placenta also converts maternal serine to glycine, which is actively transported across the foetal-placenta barrier along with alanine by transport System A (Narkewicz *et al.*, 2002; Kalhan, 2016; Fig. 6). Some foetal serine is transferred back to the placenta to form the glycine–serine shuttle, while the remaining serine and glycine can be used for foetal tissue or pyruvate synthesis. The glycine–serine shuttle and demethylation of glycine by the foetal liver provide essential one-carbon units (via *s*-adenosylmethionine) required for nucleotide synthesis and foetal growth (Lindsay

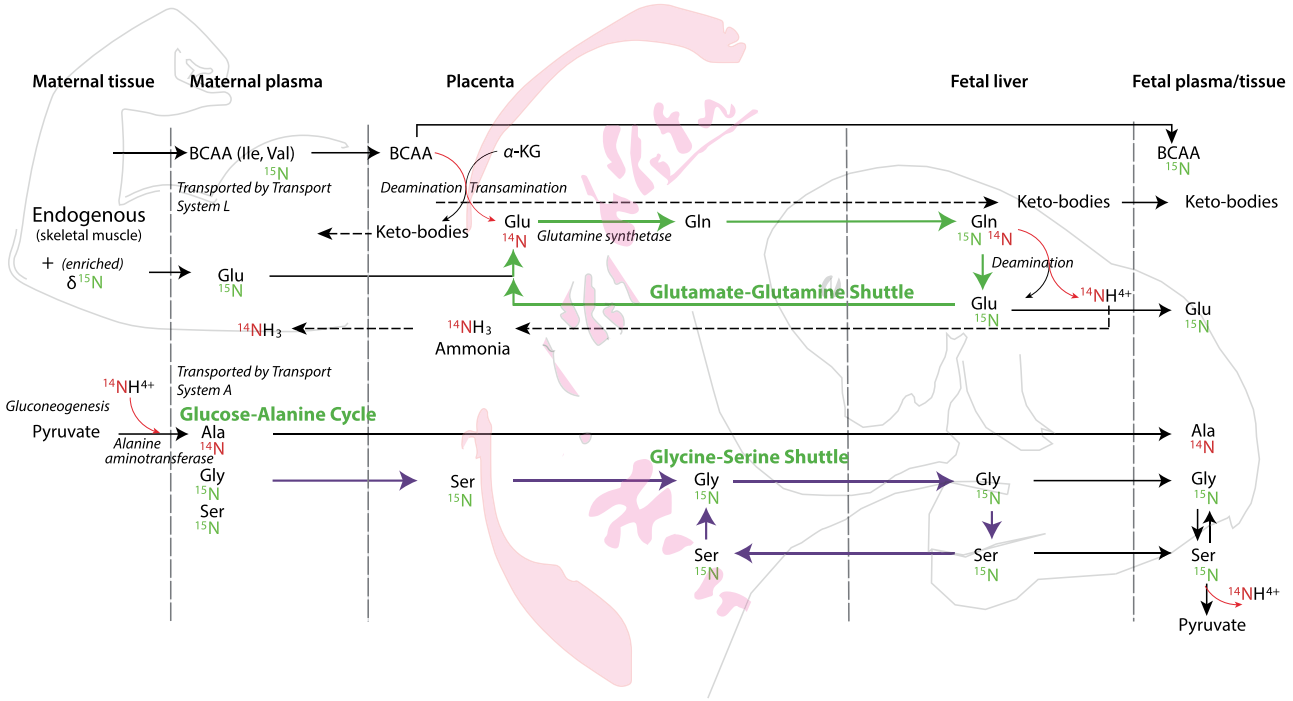

Figure 6: Maternal, placenta and foetal amino acid transfer portraying the mechanism responsible for isotopic enriched foetal δ^{15}N values. The isotopically light nitrogen (^{14}N) alanine formed when alanine aminotransferase catalyzes the synthesis of alanine from pyruvate, are transferred to the foetus (glucose–alanine cycle). The pathways by which ^{14}N are delivered to the foetus are indicated in red. Blue lines depict the glycine and serine placenta to foetal interaction (glycine–serine shuttle) while the glutamate–glutamine shuttle is indicated in green. Together with the catabolism of branched-chain amino acids (BCAA), the glutamate–glutamine shuttle delivers carbon skeletons and amino acids required for foetal development and are involved in the process of enriching the foetal δ^{15}N values. Abbreviations explanation for amino acids can be found in the Materials and methods section.

et al., 2015; Kalhan, 2016). The significantly higher (>4‰) foetal serine and glycine δ^{15}N values relative to maternal values (Fig. 5) suggest that the amine groups containing ^{14}N are preferentially deaminated to form pyruvate during this process, which leaves the remaining serine and glycine that are used to build foetal tissues ^{15}N-enriched. Ammonia containing deaminated ^{14}N is excreted from the placenta into the mother's bloodstream (plasma), leaving the heavier isotope in the foetus. This process, akin to Rayleigh distillation, could cause the observed systematic increase in foetal tissue δ^{15}N values over time (Fig. 6). It is possible that ^{14}N-enriched ammonia excreted by the foetus contributes to the preservation of maternal amino acid homoeostasis (Kalhan, 1998; De Luca *et al.*, 2012) but is more likely that this ammonia pool gets incorporated into the mother's urea cycle and is excreted via urine. Although many of these placental dynamics have primarily been described in humans (Kalhan, 2016), we expect that they are common to all placental mammals.

Glucose–alanine cycle explains mother–offspring amino acid δ^{15}N offsets

Foetal δ^{15}N alanine values were depleted on average 1.4‰ relative to their mothers, possibly driven by the glucose–alanine (Cahill) cycle. When SES are in a catabolic (fasting) state associated with negative nitrogen balance (Lübcker *et al.*, 2020), the waste nitrogen produced by amino acid catabolism in extrahepatic tissues is combined with glucose-derived carbon, yielding alanine (Felig *et al.*, 1970). This alanine is then transferred to the liver, providing a safe means of shuttling what would otherwise be dangerous nitrogen atoms (i.e. ammonium ions). Because this waste nitrogen is expected to have relatively low δ^{15}N values relative to the amino acid pool from which it originated, the newly synthesized alanine is likewise expected to have low δ^{15}N values (Lübcker *et al.*, 2020). The depleted ^{14}N-alanine in the plasma is then incorporated in tissues that are vital to maintain but will also be transferred to the foetus by transport System A. The low foetal alanine δ^{15}N values observed here therefore suggests that pregnant females are in an anabolic–catabolic physiological state during gestation (e.g. Fuller *et al.*, 2004; Habran *et al.*, 2019).

Lastly, foetal and maternal lysine and phenylalanine δ^{15}N values were similar and remained consistent during gestation. Thus, comparison of δ^{15}N in trophic (glutamic acid) and source (phenylalanine) amino acids could still provide an accurate estimate of trophic level assuming beta values and TDF for amino acids are known and do not appreciably vary

amongst individuals (Chikaraishi *et al.*, 2015). The increase in foetal threonine $\delta^{15}N$ values (+1.3‰) was offset by a decrease in maternal threonine $\delta^{15}N$ values of similar magnitude (−1.1‰). Threonine can be converted to glycine by the enzyme threonine dehydrogenase and could contribute to the maternal-to-foetal nitrogen flux (Anderson *et al.*, 1997).

Nutritional pool supporting foetal development

While SES foetal $\delta^{13}C$ values were similar to their mother's at the onset of gestation, the ^{13}C-enrichment of foetal whiskers relative to mother throughout pregnancy further confirms that foetal development is reliant on endogenous maternal protein reserves rather than maternal adipose tissue, which has significantly lower $\delta^{13}C$ values than proteinaceous tissues by 6–8‰ (DeNiro and Epstein, 1976; Tieszen *et al.*, 1983). Foetal development depends on the steady supply of glucose and catabolized endogenous maternal nitrogen (tissue proteins) from the onset of gestation. The maintenance of the maternal anabolic–catabolic state ensures a constant nutrient supply to the foetus, buffered from acute fluctuations in the mother's nutritional status during gestation. This makes sense from a maternal fitness, and perhaps evolutionary, perspective given that foetal development requires a reliable and constant supply of nutrients.

Although lactate is considered to be the main gluconeogenic precursor in fasting elephant seals and influences carbon cycling (Houser and Crocker, 2004; Champagne *et al.*, 2005; Crocker *et al.*, 2017), the glucose–alanine cycle also contributes to the maintenance of elephant seal glucose and nitrogen homoeostasis, as described above and evident through the decrease in alanine $\delta^{15}N$ values (Lübcker *et al.*, 2020). The glucose-lactate (Cori) cycle and the glucose–alanine (Cahill) cycle differ from each other in the three carbon (C_3) molecules used as intermediates and recycled to produce glucose (Dashty, 2013). The Cori cycle returns carbon to the liver as pyruvate ($C_3H_4O_3$), whereas the glucose–alanine cycle returns carbon to the liver as alanine ($C_3H_7NO_2$; Felig *et al.*, 1969). The effects of the glucose–alanine cycle on the $\delta^{15}N$ values of pregnant elephant seals have not been investigated. Potential alanine synthesis by the tricarboxylic acid (TCA) cycle is likely inadequate to replenish the plasma alanine concentrations (Felig *et al.*, 1969). It would be of interest to assess if the reported *de novo* synthesis of amino acids (e.g. glycine, serine) in fasting elephant seals could have misrepresented the actual contribution of amino acids to their glucose cycling/amount of protein sparing (e.g. Houser and Costa, 2001).

Implications and conclusions

Our study is the first to combine bulk tissue and amino acid analysis to assess whether the isotopic composition of pup tissues can be used as proxies for their mothers' isotopic composition during gestation. Contrary to the assumption that mother–offspring isotope values are positively and linearly correlated, whisker $\delta^{15}N$ and $\delta^{13}C$ values of paired, temporally overlapping mother–offspring SES were negatively correlated during gestation. It is hypothesized that the magnitude of both the nitrogen ($\Delta^{15}N$) and carbon ($\Delta^{13}C$) offset relates to foraging success and associated maternal body condition while pregnant, and caution is advised when using bulk tissue isotope values of offspring as a proxy for inferring the trophic ecology of their mothers. The observed increases in $\delta^{15}N$ values of branched-chain amino acids (valine and leucine), glycine and serine in offspring relative to their mothers, and the concurrent depletion of offspring alanine $\delta^{15}N$ values indicates that pregnant females are in a constant catabolic–anabolic state from at least the onset of gestation. Our findings shed new light on foetal amino acid metabolism, and the patterns in $\delta^{13}C$ values amongst mother and foetus confirm that foetal development primarily relies on endogenous maternal proteinaceous sources throughout gestation rather than adipose tissue. Keratinous tissue (e.g. hair) sampled from human mother–offspring pairs can similarly provide longitudinal data of foetal amino acid metabolism during pregnancy, especially when isotopically labelled one-carbon metabolites are supplemented to improve DNA methylation and promote foetal development (Kalhan, 2016).

Stable isotope analysis of offspring tissue is increasingly used to infer maternal diet selection and habitat use in free-ranging animals (Table 1). If a constant offset is assumed between offspring and maternal tissue, our results indicate that researchers could erroneously conclude that females substantially shift their resource and/or habitat use. Such misrepresentation of species ecology could mislead managers and have consequences for conservation strategies. The ecological inferences made from over two dozen studies that applied bulk tissue $\delta^{15}N$ and $\delta^{13}C$ values measured in tissues sampled from offspring of ∼30 mammal species might require reconsideration (Table 1) and potentially have serious conservation consequences. Lastly, physiological method validations that advocate minimally invasive sampling designs such as the collection of tissues from pups as proxies of their mothers' ecology should include a description of the possible limitations of this approach that are highlighted by our study.

Acknowledgements

Fieldwork was carried out under approved permits from the Animal Ethics Committee of the University of Pretoria (AUCC 040827-022, AUCC 040827-023, EC030602-016 and EC077-15). We specially thank Prof. Dan Costa [National Marine Fisheries Service (NMFS), National Oceanic and Atmospheric Administration (NOAA) Permit number 19439] for his assistance, as well as Dr Viorel Atudorei, Dr Emma Elliot Smith, Dr Grant Hall, Nicolas Prinsloo, Michael Mole and André van Tonder and other field personnel from the

Marion Island Marine Mammal Programme, University of Pretoria, South Africa. Two anonymous reviewers are thanked for their insightful comments that improved the manuscript.

Funding

This work was supported by the Society for Marine Mammalogy (SMM) Small Grant in Aid of Research, the National Research Foundation (NRF), with the logistic support of the Department of Environmental Affairs under the South African National Antarctic Program (SANAP). The conclusions drawn are attributed to the authors and not necessarily to the funders.

Data Accessibility

Data will be made available on the Dryad Digital Repository.

Authors Contributions

All authors conceived the ideas and designed methodology and enabled sample analyses. N.L., S.D.N. and J.P.W. analyzed the samples and processed the data. P.J.N.dB. maintained the fieldwork programme, facilitating access to sampling. All authors assisted with the writing of the manuscript.

Supplementary material

Supplementary material is available at *Conservation Physiology* online.

References

Anderson AH, Fennessey PV, Meschia G, Wilkening RB, Battaglia FC (1997) Placental transport of threonine and its utilization in the normal and growth-restricted fetus. *Am J Physiol Endocrinol Metab* 272: E892–E900.

Aurioles D, Koch PL, Le Boeuf BJ (2006) Differences in foraging location of Mexican and California elephant seals: evidence from stable isotopes in pups. *Mar Mammal Sci* 22: 326–338.

Bates D, Mächler M, Bolker B, Walker S (2015) Fitting linear mixed-effects models using lme4. *J Stat Softw* 67: 1–48.

Baylis AM, Orben RA, Costa DP, Arnould JP, Staniland IJ (2016) exual segregation in habitat use is smaller than expected in a highly dimorphic marine predator, the southern sea lion. *Mar Ecol Prog Ser* 554: 201–211.

Bergman JN, Bennett JR, Binley AD, Cooke SJ, Fyson V, Hlina BL, Reid CH, Vala MA, Madliger CL (2019) Scaling from individual physiological measures to population-level demographic change: case studies and future directions for conservation management. *Biol Conserv* 238: 108242.

Bester MN (1988) Chemical restraint of Antarctic fur seals and southern elephant seals. *S Afr J Wildl Res* 18: 57–60.

Birkhofer K *et al.* (2017) Methods to identify the prey of invertebrate predators in terrestrial field studies. *Ecol Evol* 7: 1942–1953.

Borrell A, Gómez-Campos E, Aguilar A (2016) Influence of reproduction on stable-isotope ratios: nitrogen and carbon isotope discrimination between mothers, fetuses, and milk in the fin whale, a capital breeder. *Physiol Biochem Zool* 89: 41–50.

Burnham KP, Anderson DR (2002) *Model Selection and Multimodel Inference: a Practical Information-Theoretic Approach*, Ed 2nd. Springer-Verlag, New York.

Champagne CD, Houser DS, Crocker DE (2005) Glucose production and substrate cycle activity in a fasting adapted animal, the northern elephant seal. *J Exp Biol* 208: 859–868.

Cherel Y, Hobson KA, Guinet C (2015) Milk isotopic values demonstrate that nursing fur seal pups are a full trophic level higher than their mothers. *RCM* 29: 1485–1490.

Chikaraishi Y, Steffan SA, Takano Y, Ohkouchi N (2015) Diet quality influences isotopic discrimination among amino acids in an aquatic vertebrate. *Ecol Evol* 5: 2048–2059.

Crocker DE, Wenzel BK, Champagne CD, Houser DS (2017) Adult male northern elephant seals maintain high rates of glucose production during extended breeding fasts. *J Comp Physiol B* 187: 1183–1192.

Dalerum F, Bennett NC, Clutton-Brock TH (2007) Longitudinal differences in ^{15}N between mothers and offspring during and after weaning in a small cooperative mammal, the meerkat (*Suricata suricatta*). *RCM* 21: 1889–1892.

Dashty M (2013) A quick look at biochemistry: carbohydrate metabolism. *Clin Biochem* 46: 1339–1352.

De Bruyn PJN, Tosh CA, Oosthuizen WC, Phalanndwa MV, Bester MN (2008) Temporary marking of unweaned southern elephant seal (*Mirounga leonina* L.) pups. *Afr J Wildl Res* 38: 133–138.

De Luca A, Boisseau N, Tea I, Louvet I, Robins RJ, Forhan A, Charles MA, Hankard R (2012) δ^{15}N and δ^{13}C in hair from newborn infants and their mothers: a cohort study. *Pediatr Res* 71: 598.

DeNiro MJ, Epstein S (1976) You are what you eat (plus a few‰): the carbon isotope cycle in food chains. *Geol Soc Amer* 6: 834–835.

Donnelly CP, Trites AW, Kitts DD (2003) Possible effects of pollock and herring on the growth and reproductive success of Steller sea lions (*Eumetopias jubatus*): insights from feeding experiments using an alternative animal model, *Rattus norvegicus*. *Br J Nutr* 89: 71–82.

Drago M, Cardona L, Aguilar A, Crespo EA, Ameghino S, García N (2010) Diet of lactating South American sea lions, as inferred from stable isotopes, influences pup growth. *Mar Mammal Sci* 26: 309–323.

Ducatez S, Dalloyau S, Richard P, Guinet C, Cherel Y (2008) Stable isotopes document winter trophic ecology and maternal investment of adult female southern elephant seals (*Mirounga leonina*) breeding at the Kerguelen Islands. *Mar Biol* 155: 413–420.

Elorriaga-Verplancken FR, Juárez-Ruiz A, Baleytó MA, Galván-Magaña F, Aguíñiga-García S (2016) Isotopic variation between adult female Guadalupe fur seals and their offspring: Implications for the use of neonates as proxies for maternal foraging. *Aquat Mamm* 42: 268–277.

Fantle MS, Dittel AI, Schwalm SM, Epifanio CE, Fogel ML (1999) A food web analysis of the juvenile blue crab, *Callinectes sapidus*, using stable isotopes in whole animals and individual amino acids. *Oecologia* 120: 416–426.

Felig P, Owen OE, Wahren J, Cahill GF (1969) Amino acid metabolism during prolonged starvation. *J Clin Investig* 48: 584–594.

Felig P, Pozefsk T, Marlis E, Cahill GF (1970) Alanine: key role in gluconeogenesis. *Science* 167: 1003–1004.

Fogel ML, Tuross N, Johnson BJ, Miller GH (1997) Biogeochemical record of ancient humans. *Org Geochem* 27: 275–287.

Fuller BT, Fuller JL, Sage NE, Harris DA, O'Connell TC, Hedges RE (2004) Nitrogen balance and δ^{15}N: why you're not what you eat during pregnancy. *RCM* 18: 2889–2896.

Gardner A, Grafen A (2009) Capturing the superorganism: a formal theory of group adaptation. *J Evol Biol* 22: 659–671.

Grecian WJ, McGill RAR, Phillips RA, Ryan PG, Furness RW (2015) Quantifying variation in δ^{13}C and δ^{15}N isotopes within and between feathers and individuals: Is one sample enough?. *Mar Biol* 162: 733–741.

Habran S, Damseaux F, Pomeroy P, Debier C, Crocker D, Lepoint G, Das K (2019) Changes in stable isotope compositions during fasting in phocid seals. *RCM* 33: 176–184.

Habran S, Debier C, Crocker DE, Houser DS, Lepoint G, Bouquegneau JM, Das K (2010) Assessment of gestation, lactation and fasting on stable isotope ratios in northern elephant seals (*Mirounga angustirostris*). *Mar Mammal Sci* 26: 880–895.

Hindell MA, Lydersen C, Hop H, Kovacs KM (2012) Pre-partum diet of adult female bearded seals in years of contrasting ice conditions. *PLoS One* 7: e38307. doi.org/10.1371/journal.pone.0038307.

Hirons AC, Schell DM, St. Aubin DJ (2001) Growth rates of vibrissae of harbor seals (*Phoca vitulina*) and Steller Sea lions (*Eumetopias jubatus*). *Can J Zool* 79: 1053–1061.

Hobson KA, McLellan BN, Woods JG (2000) Using stable carbon (δ^{13}C) and nitrogen (δ^{15}N) isotopes to infer trophic relationships among black and grizzly bears in the upper Columbia River basin, British Columbia. *Can J Zool* 78: 1332–1339.

Houser D, Costa D (2001) Protein catabolism in suckling and fasting northern elephant seal pups (*Mirounga angustirostris*). *J Comp Physiol B* 171: 635–642.

Houser DS, Crocker DE (2004) Age, sex, and reproductive state influence free amino acid concentrations in the fasting elephant seal. *Physiol Biochem Zool* 77: 838–486.

Hückstädt LA, Koch PL, McDonald BI, Goebel ME, Crocker DE, Costa DP (2012) Stable isotope analyses reveal individual variability in the trophic ecology of a top marine predator, the southern elephant seal. *Oecologia* 169: 395–406.

Jenkins SG, Partridge ST, Stephenson TR, Farley SD, Robbins CT (2001) Nitrogen and carbon isotope fractionation between mothers, neonates, and nursing offspring. *Oecologia* 129: 336–341.

Kalhan SC (1998) Protein metabolism in pregnancy. In Principles of Perinatal—Neonatal Metabolism. Springer, New York, pp 207–220.

Kalhan SC (2016) One carbon metabolism in pregnancy: impact on maternal, fetal and neonatal health. *Mol Cell Endocrinol* 435: 48–60.

Kravchenko KA, Lehnert LS, Vlaschenko AS, Voigt CC (2019) Multiple isotope tracers in fur keratin discriminate between mothers and offspring. *RCM* 33: 907–913.

Kuznetsova A, Brockhoff PB, Christensen RH (2017) lmerTest package: tests in linear mixed effects models. *J Stat Softw* 82: 1–26. https://doi.org/10.18637/jss.v082.i13.

Lerner JE, Ono K, Hernandez KM, Runstadler JA, Puryear WB, Polito MJ (2018) Evaluating the use of stable isotope analysis to infer the feeding ecology of a growing US gray seal (Halichoerus grypus) population. *PloS One* 13: e0192241. https://doi.org/10.1371/journal.pone.0192241.

Lindsay KL, Hellmuth C, Uhl O, Buss C, Wadhwa PD, Koletzko B, Entringer S (2015) Longitudinal metabolomic profiling of amino acids and lipids across healthy pregnancy. *PloS One* 10: e0145794. doi.org/10.1371/journal.pone.0145794.

Ling JK (1966) The skin and hair of the southern elephant seal, *Mirounga leonina* (Linn.) I. The facial vibrissae. *Aus J Zool* 14: 855–866.

Ling JK (2013) The skin and hair of the southern elephant seal, *Mirounga leonina* (Linn.) IV. Annual cycle of pelage follicle activity and moult. *Aus J Zool* 60: 259–271.

Lowther AD, Harcourt RG, Goldsworthy SD (2013) Regional variation in trophic ecology of adult female Australian sea lions inferred from stable isotopes in whiskers. *Wildlife Res* 40: 303–311.

Lowther AD, Goldsworthy SD (2011) Detecting alternate foraging ecotypes in Australian sea lion (*Neophoca cinerea*) colonies using stable isotope analysis. *Mar Mammal Sci* 27: 567–586.

Lübcker N, Condit R, Beltran RS, de Bruyn PJN, Bester MN (2016) Vibrissal growth parameters of southern elephant seals *Mirounga leonina*: obtaining fine-scale, time-based stable isotope data. *Mar Ecol Prog Ser* 559: 243–255.

Lübcker N, Reisinger RR, Oosthuizen WC, de Bruyn PJN, van Tonder A, Pistorius PA, Bester MN (2017) Low trophic level diet of juvenile southern elephant seals *Mirounga leonina* from Marion Island: a stable isotope investigation using vibrissal regrowths. *Mar Ecol Prog Ser* 577: 237–250.

Lübcker N, Whiteman JP, Millar RP, de Bruyn PJN, Newsome SD (2020) Fasting affects amino acid nitrogen isotope values: a new tool for identifying nitrogen balance of free-ranging mammals. *Oecologia* 193: 53–65.

Luke SG (2017) Evaluating significance in linear mixed-effects models in R. *Behav Res Methods* 49: 1494–1502.

Marshall RC, Orwin DG, Gillespie JM (1991) Structure and biochemistry of mammalian hard keratin. *Electron Microsc Rev* 4: 47–83.

McHuron EA, Holser RR, Costa DP (2019) What's in a whisker? Disentangling ecological and physiological isotopic signals. *RCM* 33: 57–66.

McInnes JC, Raymond B, Phillips RA, Jarman SN, Lea MA, Alderman R (2016) A review of methods used to analyse albatross diets—assessing priorities across their range. *Ices J Mar Sci* 73: 2125–2137.

McMahon CR, Burton HR, Bester MN (2000) Weaning mass and the future survival of juvenile southern elephant seals, *Mirounga leonina*, at Macquarie Island. *Antarct Sci* 12: 149–153.

Muggeo VM (2008) Segmented: an R package to fit regression models with broken-line relationships. *R News* 8: 20–25.

Nakagawa S, Schielzeth H (2013) A general and simple method for obtaining R^2 from generalized linear mixed-effects models. *Methods Ecol Evol* 4: 133–142.

Narkewicz MR, Jones G, Thompson H, Kolhouse F, Fennessey PV (2002) Folate cofactors regulate serine metabolism in fetal ovine hepatocytes. *Pediatr Res* 52: 589–594.

Newsome SD, Clementz MT, Koch PL (2010) Using stable isotope biogeochemistry to study marine mammal ecology. *Mar Mammal Sci* 26: 509–572.

Newsome SD, Koch PL, Etnier MA, Aurioles-Gamboa D (2006) Using carbon and nitrogen isotope values to investigate maternal strategies in northeast Pacific otariids. *Mar Mammal Sci* 22: 556–572.

Nielsen JM, Clare EL, Hayden B, Brett MT, Kratina P (2018) Diet tracing in ecology: method comparison and selection. *Methods Ecol Evol* 9: 278–291.

O'Connell TC (2017) 'Trophic' and 'source' amino acids in trophic estimation: a likely metabolic explanation. *Oecologia* 184: 317–326.

Ohkouchi N *et al.* (2017) Advances in the application of amino acid nitrogen isotopic analysis in ecological and biogeochemical studies. *Org Geochem* 113: 150–174.

Pagani-Núñez E, Renom M, Mateos-Gonzalez F, Cotín J, Senar JC (2017) The diet of great tit nestlings: comparing observation records and stable isotope analyses. *Basic Appl Ecol* 18: 57–66.

Parnell AC, Phillips DL, Bearhop S, Semmens BX, Ward EJ, Moore JW, Jackson AL, Grey J, Kelly DJ, Inger R (2013) Bayesian stable isotope mixing models. *Environmetrics* 24: 387–399.

Pauli JN, Whiteman JP, Riley MD, Middleton AD (2010) Defining noninvasive approaches for sampling of vertebrates. *Conserv Biol* 24: 49–352.

Pistorius PA, Bester MN, Kirkman SP (1999) Survivorship of a declining population of southern elephant seals, *Mirounga leonina*, in relation to age, sex and cohort. *Oecologia* 121: 201–211.

Pistorius PA, De Bruyn PJN, Bester MN (2011) Population dynamics of southern elephant seals: a synthesis of three decades of demographic research at Marion Island. *Afr J Mar Sci* 33: 523–534.

Polischuk SC, Hobson KA, Ramsay MA (2001) Use of stable-carbon and-nitrogen isotopes to assess weaning and fasting in female polar bears and their cubs. *Can J Zool* 79: 499–511.

Porras-Peters H, Aurioles-Gamboa D, Cruz-Escalona VH, Koch PL (2008) Trophic level and overlap of sea lions (*Zalophus californianus*) in the Gulf of California, Mexico. *Mar Mammal Sci* 24: 554–576.

Post DM (2002) Using stable isotopes to estimate trophic position: models, methods, and assumptions. *Ecology* 83: 703–718.

Roslin T, Majaneva S (2016) The use of DNA barcodes in food web construction—terrestrial and aquatic ecologists unite! *Genome* 59: 603–628.

Sare DT, Millar JS, Longstaffe FJ (2005) Nitrogen-and carbon-isotope fractionation between mothers and offspring in red-backed voles (*Clethrionomys gapperi*). *Can J Zool* 83: 712–716.

Scherer RD, Doll AC, Rea LD, Christ AM, Stricker CA, Witteveen B, Kline TC, Kurle CM, Wunder MB (2015) Stable isotope values in pup vibrissae reveal geographic variation in diets of gestating Steller sea lions Eumetopias jubatus. *Mar Ecol Prog Ser* 527: 261–274.

Silfer JA, Engel MH, Macko SA, Jumeau EJ (1991) Stable carbon isotope analysis of amino acid enantiomers by conventional isotope ratio mass spectrometry and combined gas chromatography/isotope ratio mass spectrometry. *Anal Chem* 63: 370–374.

Stricker CA, Christ AM, Wunder MB, Doll AC, Farley SD, Rea LD, Rosen DA, Scherer RD, Tollit DJ (2015) Stable carbon and nitrogen isotope trophic enrichment factors for Steller sea lion vibrissae relative to milk and fish/invertebrate diets. *Mar Ecol Prog Ser* 523: 255–266.

Tieszen LL, Boutton TW, Tesdahl KG, Slade NA (1983) Fractionation and turnover of stable carbon isotopes in animal tissues: implications for $\delta^{13}C$ analysis of diet. *Oecologia* 57: 32–37.

Tollit DJ, Heaslip SG, Barrick RL, Trites AW (2007) Impact of diet-index selection and the digestion of prey hard remains on determining the diet of the Steller sea lion (*Eumetopias jubatus*). *Can J Zool* 85: 1–15.

Tollit DJ, Wong MA, Trites AW (2015) Diet composition of Steller sea lions (*Eumetopias jubatus*) in Frederick Sound, southeast Alaska: a comparison of quantification methods using scats to describe temporal and spatial variabilities. *Can J Zool* 93: 361–376.

Trumble SJ, Norman SA, Crain DD, Mansouri F, Winfield ZC, Sabin R, Potter CW, Gabriele CM, Usenko S (2018) Baleen whale cortisol levels reveal a physiological response to 20th century whaling. *Nat Commun* 9: 1–8.

Whiteman JP, Elliott Smith EA, Besser AC, Newsome SD (2019) A guide to using compound-specific stable isotope analysis to study the fates of molecules in organisms and ecosystems. *Diversity* 11: 8.

Wolf JB, Harrod C, Brunner S, Salazar S, Trillmich F, Tautz D (2008) Tracing early stages of species differentiation: ecological, morphological and genetic divergence of Galpagos sea lion populations. *BMC Evol Biol* 8: 150. http://doi.org/10.1186/1471-2148-8-150.

Wu X, Xie C, Zhang Y, Fan Z, Yin Y, Blachier F (2015) Glutamate–glutamine cycle and exchange in the placenta–fetus unit during late pregnancy. *Amino Acids* 47: 45–53.

Young JW *et al.* (2015) The trophodynamics of marine top predators: current knowledge, recent advances and challenges. *Deep Sea Res Pt II* 113: 170–187.